

Projective imaging of high-energy nuclei through coherent exclusive vector meson production in electron-ion collisions

M. Kesler¹, A. I. Sheikh¹, R. Ma², Z. Tu², T. Ullrich², Z. Xu^{1,2}
¹*Department of Physics, Kent State University, Kent, OH 44240 USA and*
²*Brookhaven National Laboratory, Upton, New York 11973 USA*

(Dated: February 25, 2025)

One of the major goals of the Electron-Ion Collider (EIC) is to better understand the distributions of quarks and gluons inside nuclei at high-energy. A principal measurement is coherent exclusive vector meson (VM) production in diffractive eA collisions. The gluon spatial distribution inside the nucleus can be obtained through a Fourier transform of the nuclear momentum transfer ($|t|$) distribution for these VMs. However, the $|t|$ distribution is one of the most challenging measurements at the EIC. This research aims to overcome one of the main obstacles in this measurement: limited precision in measuring $|t|$, making it difficult to resolve the diffractive pattern from coherent events. We employ a method for reconstructing $|t|$ by utilizing the electron beam polarization in eA collisions and measuring the projected $|t|$ distribution to overcome this complication. Through the study of diffractive VM production, we carry out an experimental simulation of how the detector effect would change the extracted nuclear geometry and how to use projective techniques to avoid defects. This technique will allow us to measure the diffractive pattern in coherent events more precisely, providing a potential solution for a critical measurement that is difficult for the EIC baseline detector.

I. INTRODUCTION

The Electron-Ion Collider (EIC) has been designated as a high-priority construction project for Nuclear Physics by the Department of Energy (DOE) and Brookhaven National Laboratory (BNL) over the coming decade. As mentioned in the National Academy of Sciences report [1] and the EIC yellow report [2], mapping out the gluon distributions of nuclei and understanding the dynamics is a core mission of the EIC. A critical measurement is the exclusive diffractive vector meson (VM) production in the scattering of electrons off heavy nuclei. These events provide a clean measurement of the gluon spatial distribution in nuclei and are an effective tool for the imaging gluon spatial distributions [3]. They also serve as an excellent source for testing the intricacies of quantum chromodynamics (QCD) processes [2] and act as an experimental probe for saturation dynamics [4].

ρ mesons from photonuclear production have been measured in ultraperipheral heavy-ion collisions (UPCs) by the ALICE experiment at the Large Hadron Collider (LHC) [5] and the STAR experiment at the Relativistic Heavy-Ion Collider (RHIC) [6] to study the distribution of gluons in a heavy nucleus. However, these measurements are limited to the phase space of $Q^2 \sim 0$, where Q^2 is the virtuality of the emitted photon. To gain a more comprehensive understanding of the gluon distributions in nuclei, especially the non-linear dynamics and saturation effects, one needs to measure the VM production over a large Q^2 range down to low x (fraction of the nucleon's longitudinal momentum carried by a gluon), which can only be realized by the EIC [2]. A golden channel is through exclusive VM production, such as ρ , ω , ϕ , and J/ψ , etc, in diffractive events as depicted in Fig. 1. An electron comes in, emits a virtual photon, and scatters away. The virtual photon fluctuates into a quark-antiquark ($q\bar{q}$) pair, interacts with the nucleus

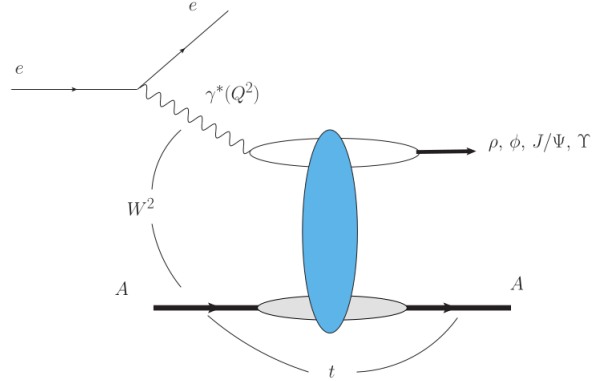


FIG. 1. Exclusive VM production in coherent diffractive $e + A$ collisions [7].

through an exchange of a Pomeron, and emerges as a VM without any other final-state particles produced in the process. At the EIC, exclusive VM production in diffractive processes constitutes a significant fraction of $e + A$ cross sections. In coherent events where the incoming nucleus remains intact, the distribution of the nuclear momentum transfer ($|t|$) reflects the spatial distribution of gluons inside the nucleus. Therefore, the gluon spatial distribution can be extracted by a Fourier transformation of the measured $|t|$ distribution. To measure this, we require a precise determination of $|t|$. However, as outlined in the ATHENA and ECCE detector proposals, measurements of exclusive VM production in $e + A$ collisions encounter two critical challenges, which could not be fully resolved in the current detector design [4, 8]: (i) the limited precision in measuring $|t|$ arising mainly from the momentum resolution of the outgoing electron, and (ii) the overwhelming incoherent background when the

nucleus breaks up.

In this work, we exploit the projected $|t|$ distribution from $e + A$ collisions. Specifically, we measure the projection of $|t|$ along the normal direction (\hat{n}) of the electron scattering plane, as shown in Fig. 3, spanned by the momenta of the incoming and outgoing electrons. Using model simulations of coherent exclusive VM production in $e + A$ collisions we quantify the impact of the EIC baseline detector performance on the measurement. We also study the sensitivity of the projected $|t|$ distribution to gluon structure in nuclei. We provide a novel approach by employing projective techniques and utilizing the electron beam polarization in $e + A$ collisions for imaging gluon distributions in nuclei for the first time in an EIC science program.

II. METHOD

The current challenges of measuring the $|t|$ distribution are illustrated in Fig. 2. The black solid line shows the typical $|t|$ distribution for coherently produced J/ψ mesons. A distinct structure of peaks and valleys is seen, where the positions of the valleys or minima are determined by the gluon distribution in the scattered nucleus, while the magnitude of the distribution is sensitive to the saturation effects. The expected $|t|$ distribution, after considering the current EIC baseline detector resolution, especially the outgoing electron's momentum resolution, is shown as blue circles. The structure of peaks and valleys is largely washed out. In addition to coherently produced VMs, there are also VMs produced in incoherent diffractive events shown as the black squares. The baseline EIC detector can significantly suppress the incoherent production, by tagging nuclear fragments on an event-by-event basis, as illustrated by the red stars. However, we are still only able to resolve the first minima. To resolve the second and third minima, another order of magnitude suppression is needed, which is extremely challenging, if not impossible. While the incoherent production is of interest on its own, it acts as an overwhelming background for measuring coherent production.

Using diffractive events in $e + A$ collisions we can directly measure the initial condition of the colliding ions, getting both momentum and spatial distributions. To access $|t|$ we need to measure the complete final state. We cannot measure the momentum of the outgoing ion, $p_{A'}$ because for heavy nuclei, the scattered nucleus remains within the beam envelope. Deriving the kinematics for A' is experimentally only possible through deeply virtual Compton scattering (DVCS) or exclusive VM production [4].

Fig. 3 shows the diagram for a coherent exclusive VM production event which is given by

$$e + A \rightarrow e' + A' + V. \quad (1)$$

Different methods of $|t| = (p_A - p_{A'})^2$ reconstruction have been used to resolve more of the diffractive pat-

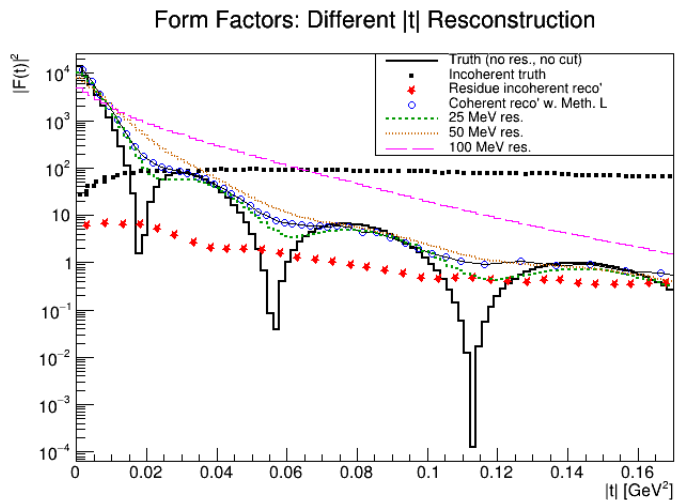


FIG. 2. Coherent and incoherent diffractive pattern in J/ψ production. The coherent truth, shown as the black solid curve, is the maximum possible diffraction pattern we can achieve. The blue circles represent the coherent $|t|$ reconstruction using Method L by the ATHENA Collaboration [4].

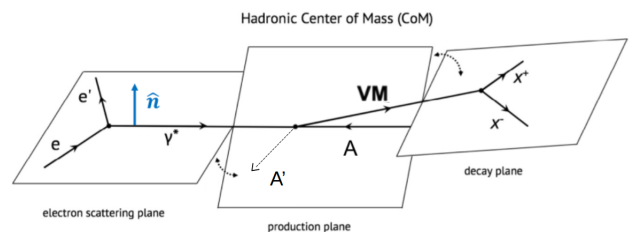


FIG. 3. Exclusive VM production in an $e + A$ collision. The normal direction to the electron scattering plane is shown as the blue arrow with \hat{n} .

tern from the coherent truth. Method E is considered the exact method, $|t| = (p_V + p_{e'} - p_e)^2$. It delivers the true $|t|$ in the absence of any distortions but it is sensitive to beam effects. Therefore, a small error, smearing, inaccuracy, etc., has a huge effect on $|t|$ and thus fails when we have beam momentum resolution. Method A is the approximate method and it involves using only the transverse momenta of the VM and the scattered electron, $|t| = (\mathbf{p}_{e'_T} + \mathbf{p}_{V_T})^2$. However, this method underestimates the true t and is only valid for small $|t|$ and small Q^2 . Method A is the only option available for incoherent events and was widely employed at HERA in diffractive VM studies. Method L relies on the invariant mass of the outgoing nucleus to establish the longitudinal momentum of the outgoing electron, rather than using the electron beam momentum [2]. It has been concluded as the best method for $|t|$ reconstruction from the EIC Yellow Report. With Method L we can experimentally determine $|t|$ through $|t| = (P_A - P_{A',corr})^2$, where P_A and $P_{A',corr}$ are the four-momenta of the incoming and outgoing nu-

clei, with the outgoing nucleus' momenta restricted by the kinematics of the coherent process. However, it applies solely to coherent events.

A. Projection Technique

To overcome the challenge of insufficient experimental resolution in resolving the diffractive pattern of the $|t|$ distribution, we propose to measure $|t|_{\hat{n}}$ instead, which is the projection of $|t|$ to the \hat{n} direction. Given that \hat{n} is perpendicular to the momentum vectors of incoming and outgoing electrons, their momenta, and thus resolutions, do not contribute. Only the electrons' flying directions before and after scattering are needed, which can be measured with much better precision than their momenta. This technique eliminates the momentum resolution contribution from the outgoing electron and we have the following

$$\begin{aligned} |t|_{\hat{n}} &= (p_V \cdot \hat{n} + p_{e'} \cdot \hat{n} - p_e \cdot \hat{n})^2 \\ &= (p_V \cdot \hat{n})^2. \end{aligned} \quad (2)$$

Figure 3 displays exclusive VM production in a coherent event, where e and e' denote incoming and outgoing electrons, γ^* represents the emitted virtual photon, A is the incoming nucleus, and **VM** indicates the produced VM that decays into X^+ and X^- [9]. The blue vertical arrow points to the normal direction (\hat{n}) of the electron scattering plane, spanned by the momenta of incoming and outgoing electrons.

For heavy-ions, the form factor can be given by the convolution of the Yukawa potential with the Woods-Saxon distribution approximated as a hard sphere potential [9, 10] which is given by

$$F(t) = \frac{4\pi\rho_0}{Aq^3} [\sin(tR) - tR \cos(tR)] \left(\frac{1}{1 + a^2t^2} \right), \quad (3)$$

where $t = q^2$ is the nuclear momentum transfer, ρ_0 is the central density, A is the atomic mass number, R is the nuclear radius, and the range of the Yukawa potential is given by $a = 0.7$ fm.

The Mandelstam variable t can be decomposed as

$$t = t_{\perp} + t_{\parallel}, \quad (4)$$

where $t_{\perp} = t_x + t_y$. We further decompose the perpendicular components normal to the electron scattering plane and call one the normal direction i.e. t_y . Given that $t_{\perp} = q_{\perp}^2 = q_x^2 + q_y^2$, we can parameterize t_{\perp} in terms of q_{\perp} giving

$$q_x = q_{\perp} \sin(\theta_{\max}), \quad q_y = q_{\perp} \cos(\theta_{\max}). \quad (5)$$

We can now cut a wedge of angle θ_{\max} from the \hat{n} -direction, i.e. q_y , to eliminate most of the q_x component which is responsible for the outgoing electrons momentum resolution contribution.

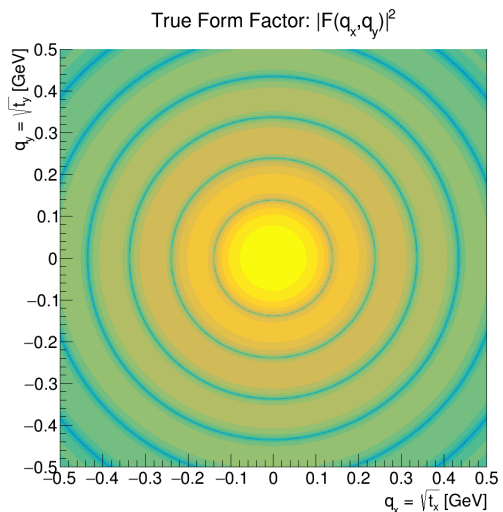


FIG. 4. 2D-phase space of the form factor from Eq. 3 with no cut or resolution added.

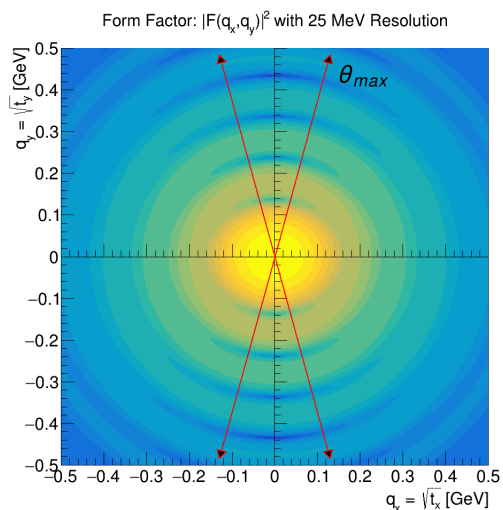


FIG. 5. Form factor from Eq. 3 in 2D-phase space with a wedge cut of $\theta_{\max} = \pi/12$ from the $q_y = \sqrt{t_y}$ -axis and an added resolution of 25 MeV. Here we see that the shape is more elliptical due to the detector resolution.

III. RESULTS

Simulations have been developed to add detector resolution to the form factor by convoluting Eq. 3 with a Gaussian. Figure 4 shows the form factor from Eq. 3 as a function of $q_x = \pm\sqrt{t_x} = (p_V + p_{e'} - p_e) \cdot (\hat{n} \times \hat{z})$ and $q_y = \pm\sqrt{t_y} = p_V \cdot \hat{n}$. We can see the symmetric nature of the form factor when no detector resolution is added. Upon adding resolution to the form factor, $|F(t = q^2)|^2$, our distribution will become more elliptical due to the smearing, as seen in Figure 5. The distortion escalates with increasing resolution and angle cut θ_{\max} . The optimal wedge selection of θ_{\max} depends on the detector $|t|$ resolution and the experimental statistics. This

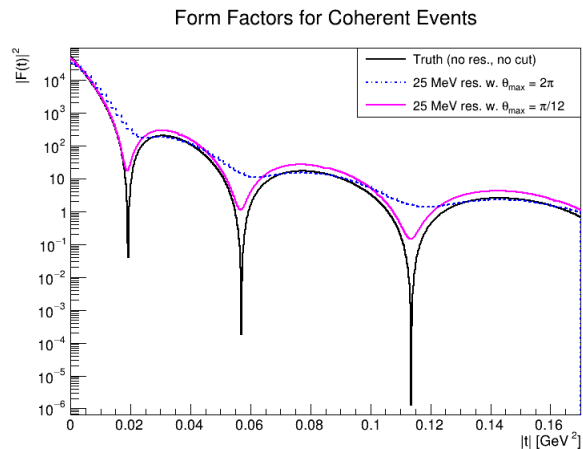


FIG. 6. $|t|$ distribution for coherent VM production. The coherent truth is shown as the black curve. We have added 25 MeV resolution to the blue and magenta curves. The blue curve shows the diffractive pattern when we take into account the entire $\theta_{\max} = 2\pi$ phase-space and the magenta curve is with a wedge cut of $\theta_{\max} = \pi/12$.

parameter could be optimized in the realistic detector configuration.

In order to illustrate the feasibility of this technique, a realistic $|t|$ resolution of $\sigma_{\sqrt{|t|}} = 25\text{MeV}$ is chosen. This was obtained by convoluting the form factor with different $|t|$ resolutions and comparing to the ATHENA detector simulation shown in Fig. 2. The Method L reconstruction from the ATHENA detector configuration seems to be compatible with a $|t|$ resolution between 25-50 MeV. Therefore, we have chosen 25 MeV for our plot to compare adding resolution to no wedge cut, i.e. the entire phase space ($\theta_{\max} = 2\pi$), with a cut of $\theta_{\max} = \pi/12$. The result of our projection technique on the $|t|$ distribution is shown in Fig. 6. We can see a significant improvement in resolving the diffractive pattern of the $|t|$ distribution.

IV. DISCUSSION

In future work, we will use the RooUnfold package [11] to analyze how much of the true cross section we can recover and study the feasibility of this strategy. This will allow us to quantify the best angle θ_{\max} to use for our proposed technique. We will also test this method on EIC and ePIC software [12].

Additionally, we plan to implement the decay pattern of the VM with respect to \hat{n} to accurately determine the fraction of coherently produced VMs by utilizing the transversely polarized electron beams, i.e., the electron spin is perpendicular to its momentum.

In coherent events, where the incoming electron flips its spin after scattering, the spin of the produced VM will align with \hat{n} , as shown in Fig. 7. This results in a non-trivial pattern, while such an alignment is absent for incoherently produced VMs. The spin of the emitted

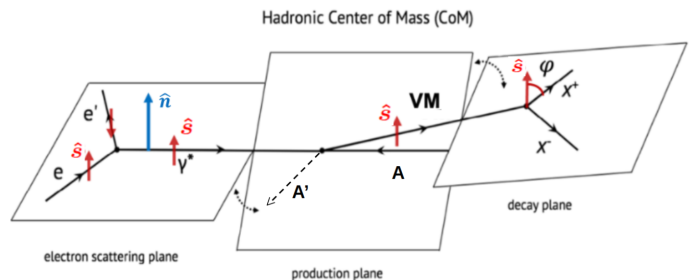


FIG. 7. Coherent exclusive VM production in an $e + A$ collision. The spin directions are shown as red arrows with \hat{s} .

virtual photon aligns with the spin of the incoming electron, given that the exchanged Pomeron has 0 spin, and finally transfers to the produced VM. In other words, the spin of the VM will align with \hat{n} . If then the momentum of the VM's decay daughter is projected onto the VM's spin direction, \hat{s} (i.e., \hat{n}), a $\cos(2\phi)$ modulation is expected [13]. However, if the spin of the incoming electron does not flip, there will be no preferred direction for the spin of the virtual photon or the VM, and a flat distribution ϕ is expected. Similarly, in incoherent events, the spin of the VM is expected to be random with respect to \hat{n} , and therefore no modulation $\cos(2\phi)$ should be observed. Consequently, the fraction of coherent events, in which the incoming electron flips its spin, is equal to $\langle \cos(2\phi) \rangle$, where the average runs over all exclusive VM events. If we assume that the probability for the incoming electron to flip its spin is C , which is expected to be independent of $|t|_{\hat{n}}$ since they are causally disconnected, the fraction of total coherent events will be $\langle \cos(2\phi) \rangle / C$. By measuring such a fraction in each $|t|_{\hat{n}}$ bin, one can obtain the $|t|_{\hat{n}}$ distributions for coherent VM production. From this the spatial distribution of the gluons in the nucleus can be extracted. As a by-product, one can also obtain the incoherent exclusive VM cross section as a function of $|t|_{\hat{n}}$ and study fluctuations in the gluon density.

In summary, we demonstrated a unique approach to measure the projected $|t|$ distribution and propose to separate coherent and incoherent production by exploiting the electron beam polarization for imaging the gluon distribution in the nucleus at the EIC. This method provides a possible solution for the mission-critical measurement of exclusive VM production in $e + A$ collisions, which is rather challenging, if not impossible, for the EIC baseline detector. This work could significantly enhance the scientific output of the EIC and is the first physics program to utilize electron beam polarization in $e + A$ collisions. We aim to derive a standard analysis tool for spin-based projective imaging for future applications at colliders.

ACKNOWLEDGMENTS

This research is supported by the US Department of Energy, Office of Nuclear Physics (DOE NP), under contract Nos. DE-FG02-89ER40531, DE-SC0012704.

-
- [1] National Academies of Sciences, Engineering, and Medicine, An Assessment of U.S.-Based Electron-Ion Collider Science (The National Academies Press, Washington, DC, 2018).
- [2] R. Abdul Khalek et al., Science Requirements and Detector Concepts for the Electron-Ion Collider: EIC Yellow Report, Nucl. Phys. A **1026**, 122447 (2022), arXiv:2103.05419 [physics.ins-det].
- [3] A. Caldwell and H. Kowalski, Investigating the gluonic structure of nuclei via J/ψ scattering, Phys. Rev. C **81**, 025203 (2010).
- [4] J. Adam et al. (ATHENA), ATHENA detector proposal — a totally hermetic electron nucleus apparatus proposed for IP6 at the Electron-Ion Collider, JINST **17** (10), P10019, arXiv:2210.09048 [physics.ins-det].
- [5] S. Acharya et al. (ALICE), Coherent photoproduction of ρ^0 vector mesons in ultra-peripheral Pb-Pb collisions at $\sqrt{s_{NN}} = 5.02$ TeV, JHEP **06**, 035, arXiv:2002.10897 [nucl-ex].
- [6] L. Adamczyk et al. (STAR), Coherent diffractive photoproduction of ρ^0 mesons on gold nuclei at 200 GeV/nucleon-pair at the Relativistic Heavy Ion Collider, Phys. Rev. C **96**, 054904 (2017), arXiv:1702.07705 [nucl-ex].
- [7] M. Krelina, V. P. Goncalves, and J. Cepila, Coherent and incoherent vector meson electroproduction in the future electron-ion colliders: the hot-spot predictions, Nucl. Phys. A **989**, 187 (2019), arXiv:1905.06759 [hep-ph].
- [8] J. K. Adkins et al., Design of the ECCE detector for the Electron Ion Collider, Nucl. Instrum. Meth. A **1073**, 170240 (2025), arXiv:2209.02580 [physics.ins-det].
- [9] M. Lomnitz and S. Klein, Exclusive vector meson production at an electron-ion collider, Phys. Rev. C **99**, 015203 (2019), arXiv:1803.06420 [nucl-ex].
- [10] T. Toll and T. Ullrich, Exclusive diffractive processes in electron-ion collisions, Phys. Rev. C **87**, 024913 (2013), arXiv:1211.3048 [hep-ph].
- [11] H. B. Prosper and L. Lyons, eds., CERN Yellow Reports: Conference Proceedings (CERN, Geneva, 2011).
- [12] E. U. Group and ePIC Collaboration, (2023).
- [13] M. Abdallah et al. (STAR), Tomography of ultrarelativistic nuclei with polarized photon-gluon collisions, Sci. Adv. **9**, eabq3903 (2023), arXiv:2204.01625 [nucl-ex].
- [14] M. Lomnitz, Coherent vector meson production at an electron ion collider, PoS **DIS2018**, 171 (2018), arXiv:1805.08586 [nucl-ex].
- [15] S. Klein and J. Nystrand, Exclusive vector meson production in relativistic heavy ion collisions, Phys. Rev. C **60**, 014903 (1999), arXiv:hep-ph/9902259.
- [16] A. Accardi et al., Electron Ion Collider: The Next QCD Frontier: Understanding the glue that binds us all, Eur. Phys. J. A **52**, 268 (2016), arXiv:1212.1701 [nucl-ex].
- [17] An Assessment of U.S.-Based Electron-Ion Collider Science (National Academies Press, 2018).